### **Rotating Skyrmion Stars**

Rachid OUYED

Nordic Institute for Theoretical Physics, Blegdamsvej 17, DK-2100 Copenhagen, Denmark

Received/Accepted

Abstract. In a previous paper, using an equation of state of dense matter representing a fluid of Skyrmions we constructed the corresponding non-rotating compact-star models in hydrostatic equilibrium; these are mostly fluid stars (the Skyrmion fluid) thus naming them Skyrmion Stars. Here we generalize our previous calculations by constructing equilibrium sequences of rotating Skyrmion stars in general relativity using the computer code RNS developed by Stergioulas. We calculated their masses and radii to be  $0.4 \le M/M_{\odot} \le 3.45$ , and  $13.0 \text{ km} \le R \le 23.0 \text{ km}$ , respectively (R being the circumferential radius of the star). The period of the maximally rotating Skyrmion stars is calculated to be  $0.8 \text{ ms} \le P \le 2.0 \text{ ms}$ . We find that a gap (the height between the star surface and the inner stable circular orbit) starts to appear for  $M \sim 2.0 M_{\odot}$ . Specifically, the Skyrmion star mass range with an existing gap is calculated to be  $1.8 < M/M_{\odot} < 3.0$  with the corresponding orbital frequency  $0.8 \text{ kHz} < \nu_{\rm ISCO} < 1.3 \text{ kHz}$ . We apply our model to the 4U 1820-30 low mass X-ray binary and suggest a plausible Skyrmion star candidate in the 4U 1636-53 system. We discuss the difficulties encountered by our model in the 4U 0614+09 case with the highest known Quasi-Periodic Oscillation frequency of 1329 Hz. A comparative study of Skyrmion stars and models of neutron stars based on recent/modern equations of state is also presented.

Key words. dense matter - equation of state - stars: compact - stars: rotation

### 1. Introduction

A key input in determining the structure of compact objects is the equation of state (EOS) of high density matter whose determination remains a formidable theoretical problem. There is no general agreement still on the exact composition of dense matter, and on its EOS, especially for densities in excess several times nuclear matter density (in a regime where the EOS is poorly constrained by nuclear data and experiments). In Ouved & Butler (1999, hereafter OB), we presented and discussed the Skyrme model (Skyrme 1962a&b) and its plausible link to Quantum Chromo-Dynamics (QCD). We explained how the connections are intriguing enough that the model has been revived in order to study its predictions of hadronic interactions. Following an approach outlined in Kälbermann (1997), we thus constructed an equation of state of dense matter which describes a fluid of Skyrmions coupled to a dilaton field (associated with the glueball of QCD) and a vector meson field (coupled to the baryon number). Using our code, we constructed non-rotating, zero-temperature stable compact objects – we called Skyrmion Stars – and calculated their masses and radii to be  $0.4 \leq M/M_{\odot} \leq 2.95$  and 11.0 km  $\leq$  $R \leq 15.3$  km, respectively. In §5.1 in OB we compared Skyrmion stars – as defined in our model – to other

"Exotic" stars which also follow from solutions to an effective non-linear field theory of strong forces (see also Heusler, Droz, & Straumann 1992 and references therein). Skyrmion stars in our picture are not boson/soliton stars where the soliton is a global structure over the scale of the star but rather form their constituent baryons as topological solitons using pions fields.

In this paper, we compute models of rotating Skyrmion stars using the RNS code written and made publicly available by N. Stergioulas (Stergioulas & Friedman 1995). RNS constructs models of rapidly rotating, relativistic, compact stars and assumes uniform rotation. The computation solves for the hydrostatic and Einstein field equations for uniformly rotating mass distributions, under the assumptions of stationarity, axial symmetry about the rotation axis, and reflection symmetry about the equatorial plane. The paper is presented as follows: In §2, we describe the equations solved by the RNS code and then construct the corresponding rotating Skyrmion stars. The results are analyzed and discussed in §3. A comparative study of Skyrmion stars and neutron stars is done in §4 before concluding in §5.

### 2. Rapidly and rigidly rotating relativistic Skyrmion stars

Here we present a brief outline of the equations solved for by the RNS code. We start by describing the space-time

around a rotating compact star in quasi-isotropic coordinates, as a generalization of Bardeen's metric (Bardeen 1970):

$$ds^{2} = -e^{\gamma + \rho} dt^{2} + e^{2\alpha} (r^{2} d\theta^{2} + dr^{2})$$

$$+ e^{\gamma - \rho} r^{2} \sin(\theta)^{2} (d\phi - \omega dt)^{2}.$$
(1)

(c=1=G). The metric potentials,  $\gamma$ ,  $\rho$ ,  $\alpha$ , and the angular velocity of the stellar fluid to the relative local inertial frame  $(\omega)$  are all functions of the quasi-isotropic radial coordinates (r) and the polar angle  $(\theta)$ . The function  $(\gamma+\rho)/2$  is the relativistic generalization of the Newtonian gravitational potential; the time dilation factor between an observer moving with angular velocity  $\omega$  and an observer at infinity is  $\exp(1/2(\gamma+\rho))$ . We investigate uniformly rotating perfect fluid stars with the energy momentum tensor given by:

$$T^{\mu\nu} = (\epsilon + P)u^{\mu}u^{\nu} + Pg^{\mu\nu} , \qquad (2)$$

where  $\epsilon$  is the total energy density, P the pressure and  $u^{\mu}$  the unit time-like four velocity vector that satisfies

$$u^{\mu}u_{\mu} = -1. \tag{3}$$

The proper velocity v of the matter, relative to the local Zero Angular Momentum Observer (ZAMO), is given in terms of the angular velocity  $\Omega \equiv u^3/u^0$  of the fluid element (measured by a distant observer in an asymptotically flat space-time), by the following equation:

$$v = (\Omega - \omega)r\sin(\theta)e^{-\rho} . \tag{4}$$

The four velocity  $(u^{\mu})$  of the matter can be written as

$$u^{\mu} = \frac{e^{-(\gamma+\rho)/2}}{(1-v^2)^{1/2}}(1,0,0,\Omega) \ . \tag{5}$$

Substitution of the above equation into Einstein field equations projected on to the frame of reference of a ZAMO yield three elliptic equations for the metric potentials  $\rho$ ,  $\gamma$  and  $\omega$  and two linear ordinary differential equations for the metric potential  $\alpha$  (Bardeen 1971; Butterworth, & Ipser 1976; Komatsu, Erigushi, & Hachisu 1989). In general, the elliptic differential equations are converted to integral equations for the metric potentials using Green's function approach.

From the relativistic equations of motion, the equation of hydrostatic equilibrium for a barytropic fluid (the field equations are integrated by assuming various zero-temperature, barotropic EOS of the form  $\epsilon = \epsilon(p)$ ) may be obtained as:

$$h(P) - h_{\rm p} = \frac{1}{2} [\gamma_{\rm p} + \rho_{\rm p} - \gamma - \rho - \ln(1 - v^2) + A^2 (\omega - \Omega_{\rm c})^2], \qquad (6)$$

where h(P) is termed as the specific enthalpy.  $P_{\rm p}$  is the rescaled values for pressure, and  $h_{\rm p}$  is the specific enthalpy at the pole.  $\gamma_{\rm p}$  and  $\rho_{\rm p}$  are the values of the metric potentials at the pole, and  $\Omega = r_{\rm e}\Omega$ . A is a rotation constant (Komatsu, Erigushi, & Hachisu 1989) and the subscripts,

p, e and c stand for polar, equatorial and central, respectively. RNS solves the integral equation for  $\rho$ ,  $\gamma$  and  $\omega$ , the ordinary differential equation (in  $\theta$ ) for the metric potential  $\alpha$ , together with Eq. (6), the hydrostatic equilibrium equations at the center  $[h(P_c)$  given] and at the equator  $[h(P_e) = 0]$ , iteratively to obtain  $\rho$ ,  $\gamma$ ,  $\alpha$ ,  $\omega$ , the equatorial coordinate radius  $(r_e)$ , angular velocity  $(\Omega)$ , and the density  $(\epsilon)$  and pressure (P) profiles.

The geodesic motion for circular orbits around rotating relativistic stars is also presented in Bardeen (1970) and correspond to the motion of ZAMO yielding two possible values for the velocity corresponding to corotating and counter-rotating orbits. The innermost stable circular orbits are given by solving for V, rr = 0 where V is the effective potential as written in Bardeen (1972); the comma followed by rr represent a second order partial derivative with respect to radius r.

### 3. Numerical results

### 3.1. Maximally rotating configurations

The highest energy density used in all the computed rotating models is the value which gives the maximum mass non-rotating star as calculated in OB. We specify the equation of state, and the central energy density and the code computes models with increasing angular velocity until the star is spinning with the same angular velocity as a particle orbiting the star at its equator<sup>1</sup>.

Fig. 1a and 1b show the resulting stellar masses and radii as a function of the central density, respectively. The mass range is  $0.4 \le M/M_{\odot} \le 3.45$  while the corresponding radii (equatorial circumferential radius; [proper equatorial circumference]/ $2\pi$ ) are calculated to be 18.6 km  $\leq$ R < 23.0 km. In Fig. 1c, we show the resulting Mass-Radius plane. In general, for a given central density, rotation allows the masses and radii to increase by 30 % and 40%, respectively, when compared with the non-rotating cases. The amount of baryonic mass in the outer region of the star (the crust region where  $\rho < \rho_{\rm N}$  is constructed using the EOS of Baym, Pethick, & Sutherland (1971);  $\rho_N$  is the nuclear saturation density) decreases drastically with rotation. Rotating Skyrmion stars crust constitute less than 5% of the total baryonic mass while it averages 20% for the static configurations. The nuclear crust is further addressed in OB to which we refer the interested reader.

The minimum spin period as a function of mass is shown in Fig. 2a and is calculated to be 0.8 ms  $\leq P \leq$  2.0 ms. The inertial frame dragging at the center of the star to the rotation rate is plotted in Fig. 2b which shows a significant value throughout and reaches a maximum value of 0.8 for the most massive stars. It suggests that frame-dragging might have a significant effect on the structure

<sup>&</sup>lt;sup>1</sup> We will sometimes refer to it as the Kepler frequency which is the frequency of a particle in a stable orbit at the circumference of a star. It is therefore also the frequency at which disruption of the star would occur.

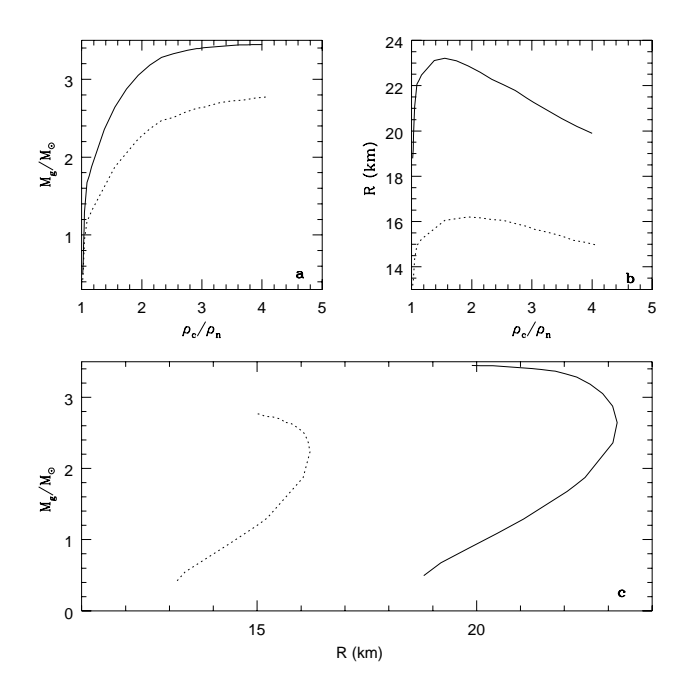


Fig. 1. Maximally rotating configurations: a). Gravitational Mass versus central density (in units of the nuclear saturation density) for zero temperature Skyrmion stars in hydrostatic equilibrium. In this figure, the solid curves represent the rotating configurations while the dotted curves represent the non-rotating or static configurations. b). Radius versus central density. c). The Mass—Radius plane.

of rotating Skyrmion stars as P decreases since it is taking place against the background of a radially dependent, frame-dragging frequency (see Weber & Glendenning 1992 for example).

It has been noted by Hænsel & Zdunik (1989) and Friedman & Ipser (1992) that the maximum spin rate for many neutron star EOS seems to be given by

$$\Omega_{max} = \chi \left(\frac{M_{\text{s,max.}}}{M_{\odot}}\right)^{1/2} \left(\frac{R_{\text{s,max.}}}{10 \text{ km}}\right)^{-3/2} \quad s^{-1} , \qquad (7)$$

where  $\chi$  has been quoted as either 7600 or 7700  $s^{-1}$ .  $M_{\rm s,max.}$  and  $R_{\rm s,max.}$  are the total mass-energy and areal radius of the maximum-mass static configuration for a given EOS. The newest fit for the proportionality constant can be found in Haensel, Salgado, & Bonazzola (1995) where  $\chi = 7600-7900~\rm s^{-1}$  is given. If we assume that the minimum spin period for the Skyrmion star is 0.8 ms (that is the star with the maximum mass on the Kepler sequence has the maximum rotation rate) then the maximum angular velocity is 7854 rad  $s^{-1}$ . Using the values for the maximum mass spherical star we get,

$$\Omega_{max} = 7600 - 7900 \times (2.95)^{1/2} (1.44)^{-3/2} 
= 7555 - 7852 s^{-1}.$$
(8)

This corresponds to less than few percent error which makes Eq. (7) an excellent tool for predicting the maximum angular velocity even for our EOS.

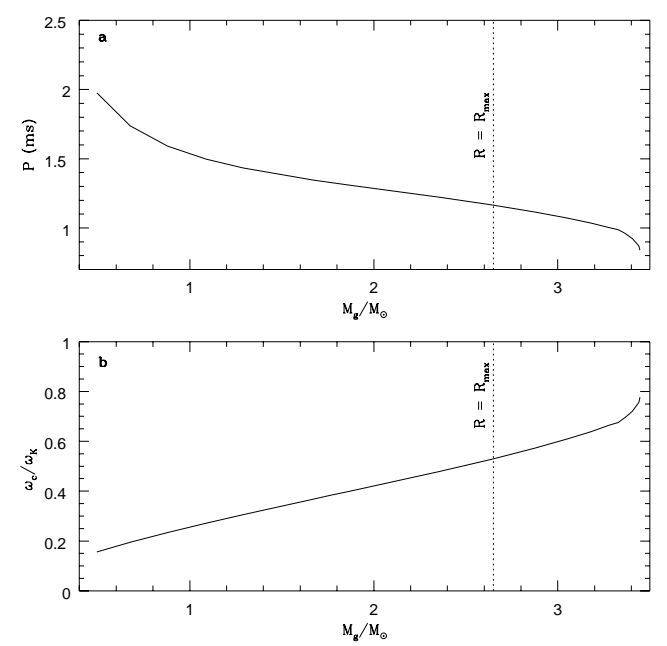


Fig. 2. Maximally rotating configurations: a). Period versus gravitational mass for zero temperature Skyrmion stars in hydrostatic equilibrium. b). Ratio of the inertial frame dragging at the center of the star to the rotation rate versus gravitational mass. In this Figure and the subsequent ones, the vertical dotted line illustrates the mass of the maximum radius configuration.

The centrifugal flattening of maximally rotating Skyrmion stars is obvious from Fig. 3a with eccentricities  $e = \sqrt{1-(R_p/R_e)^2}$  ( $R_p$  and  $R_e$  being the polar and equatorial radius of the configuration, respectively) ranging from 0.78 for the lightest stars up to 0.86 for the heaviest ones. The maximum eccentricity is reached at  $M=2.62M_{\odot}$  (the maximum radius configuration) after which e decreases, as expected. Fig. 3b shows the Kinetic to gravitational energy ratio (T/|W|) versus gravitational mass. Configurations with T/|W| above the dashed line might be unstable to the bar mode. We come back to this in §3.2 where we discuss the conditions for the onset of non-axisymmetric modes and to what extent they could be used as a stronger constraint than the maximum rotational frequency.

In Fig. 4, the moment of inertia (Fig. 4a) and the angular momentum (Fig. 4b) are plotted. The sudden decrease in the moment of inertia for  $M \geq 3.3 M_{\odot}$  is the consequence of the mass reaching a "plateau" (at  $M=3.3 M_{\odot}$ ) while the radius keeps decreasing (see Fig. 1a and Fig. 1b). The combined effects of I decreasing with  $\Omega$  increasing (Fig. 2a) explains then why the angular momentum stays constant for  $M \geq 3.3 M_{\odot}$  - using the simple dimensional analysis  $J = I\Omega$ . Finally the height from surface of the

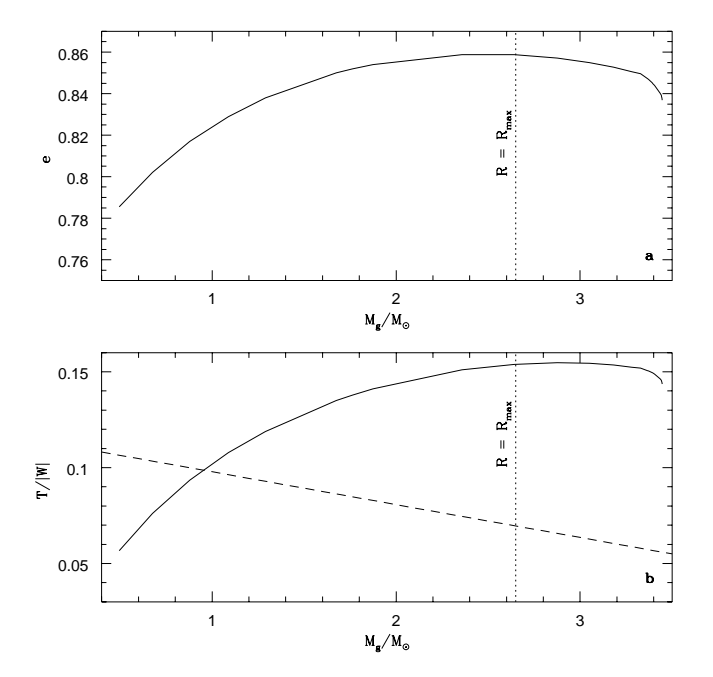


Fig. 3. Maximally rotating configurations: a). Eccentricity versus gravitational mass for zero temperature Skyrmion stars in hydrostatic equilibrium. b). Kinetic to gravitational energy ratio versus gravitational mass. The dashed line is based on the empirical formula for the onset of the bar mode instability as described by Eq.9. Configurations with T/|W| above the dashed line might be unstable to the bar mode.

last stable co-rotating orbit  $(h_+ = r_{\rm orb.} - R)^2$  is shown in Fig. 4c. It can be seen from this figure that in general the stable orbits exists up to the surface of the star. The large radii calculated makes it very difficult for the stable orbit to be outside the star (when compared to  $6GM/c^2$ ; the inner most stable Kepler orbit around the non-rotating case). For the most massive configurations  $(M \geq 3.2 M_{\odot})$ , the boundary layer (the separation between the surface of the neutron star and its innermost stable orbit) can be as as high as 1.5 km for the maximum value. Lowering the spin frequency will eventually relax the above conclusions (see §3.3).

### 3.2. Bar instability

Skyrmion stars are subject to rotational constraints linked to gravitational-wave instabilities which make all rotating, perfect fluid equilibria unstable to modes with angular dependence  $\exp(im\phi)$  for sufficiently large m (Friedman & Schutz 1978; Lindblom 1984). These instabilities allow the star to convert its rotational energy to gravitational energy waves (Glendenning 1997).

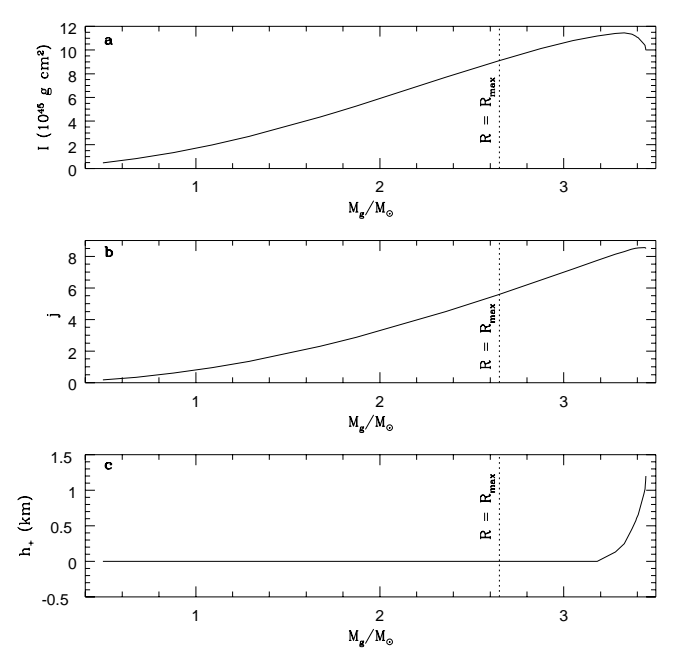


Fig. 4. Maximally rotating configurations: a). Moment of inertia versus gravitational mass for zero temperature Skyrmion stars in hydrostatic equilibrium. b). Angular momentum (Dimensionless ratio of angular momentum  $cJ/GM_{\odot}^2$ ) versus gravitational mass. c). Height from surface of last stable co-rotating orbit in equatorial plane versus gravitational mass.

Fairly recent general relativistic calculations have shown that the gravitational-radiation-driven bar-mode (f-mode) instability sets in at values of T/|W| much lower than in the Newtonian limit. For the case of realistic EOS, Morsink, Stergioulas, & Blattnig (1999) found the following empirical formula for the onset of the bar mode instability (the case of polytropes can be found in Stergioulas & Friedman 1998):

$$T/|W| = 0.115 - 0.048M/M_{max}^{sph}$$
, (9)

where  $M_{max}^{sph}$  is the maximum mass star for the non-rotating case. Assuming that this formula holds for our EOS, we find that all maximally rotating stars with  $M \geq M_{\odot}$  might be prone to such an instability.

The real question, however, is whether the f-mode instability is actually going to limit the spin period of Skyrmion stars. With the onset of the m=2 (f-mode), the r-mode<sup>3</sup> will soon become unstable (Friedman & Morsink 1998) and spin down the star to even slower rate. As a result, it is not expected that the f-mode will limit the spin-rate of any stars (Andersson, Kokkotas, & Schutz

 $<sup>^2</sup>$  For the cases where  $r_{\rm orb.}$  is non-existent or inside the star,  $r_{\rm orb.}$  is taken to be the Keplerian orbit radius at the surface of the star.

 $<sup>^3</sup>$  The r-mode instability is a member of the class of gravitational-radiation-driven instabilities and are generic in rotating neutron stars (Friedman & Morsink 1998). That is, every r-mode is in principle unstable in every rotating star, in the absence of viscosity.

1999), although it may become unstable and emit gravitational radiation in some cases.

### 3.2.1. Skyrmion fluid viscosity

Realistic compact stars are viscous, and the presence of viscosity will shift the onset of instability and if large enough will damp out the instability (Andersson, Kokkotas, & Schutz 1999). If the instability is driven by viscous dissipation, it was shown in Bonazzola, Frieben, & Gourgoulhon (1995) that for cold uniformly rotating NS only very stiff equations of state are likely to allow for spontaneous symmetry breaking. If we consider the stiffness of our EOS (when compared to standard EOS; see Figure 2 in OB) then instability to a bar mode is a very likely plausibility in Skyrmion stars. So how viscous is a Skyrmion fluid and what is its temperature dependency?

The Skyrmion fluid can be looked at as made of fermionic soliton objects and in principle one should be able to calculate its physical parameters, among others its viscosity. The complication is linked to the fact that unlike a pure fermionic fluid, the structure of the Skyrmion fluid is highly non-linear (a consequence of the Skyrmion having structure). This makes the calculations not trivial and beyond the scope of this paper. There might still be the possibility that such a fluid is viscous enough that it will of course damp these instabilities altogether so that limits on rotation is set by the Kepler frequency - a notion to be confirmed.

# 3.3. Different spin frequencies: Skyrmion stars and QPOs

The discovery of kilohertz Quasi-Periodic Oscillations (QPOs) in low mass X-ray binaries (LMXBs) with the Rossi X-Ray Timing Explorer has stimulated extensive studies of these sources (van der Klis 1998). One thing that has been suggested in the literature is that the highest frequency QPO observed could correspond to the orbital frequency at the inner stable circular orbit (ISCO) (Miller, Lamb, & Psaltis 1998). The signature of the marginally stable orbit is a saturation in QPO frequency (assumed to track inner disk radius) versus mass accretion. Such a saturation where the frequency becomes independent of the chosen mass accretion rate indicator has been reported in 4U 1820-30 (Zhang et al. 1998; Kaaret et al. 1999).

In Fig. 5a we plotted ISCO frequency (for the prograde case only) versus Mass for Skyrmion star models rotating at frequencies 290, 360 and 580 Hz respectively. These values allow us to cover the range of frequencies observed in LMXBs. Fig. 5b shows the corresponding gaps; that is the height between the star surface and the ISCO (prograde case). In general, the Skyrmion star mass range with an existing gap is calculated to be,

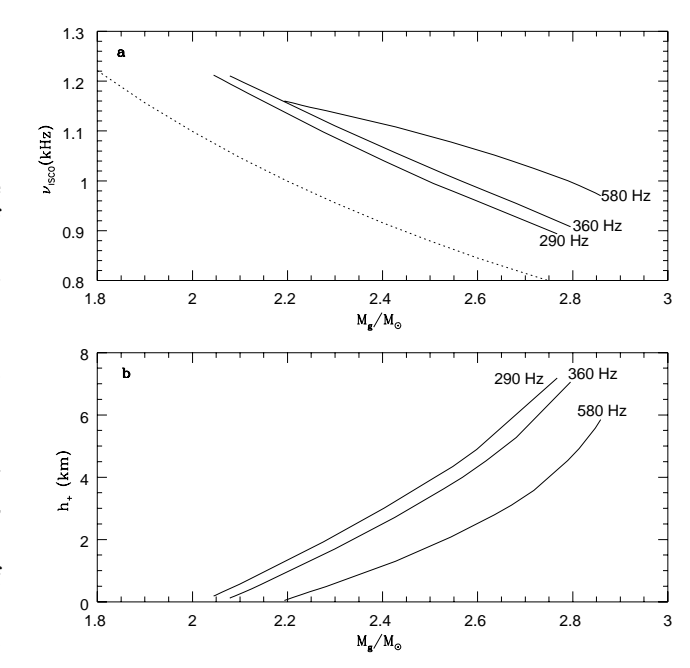


Fig. 5. Different spin frequencies: a). The ISCO frequency versus mass for Skyrmion stars rotating at 290, 360 and 580 Hz respectively. The dotted line represents the static models,  $\nu_{ISCO} = 2198 \text{ Hz}(M_{\odot}/M)$ . b). Height from the star surface of the innermost stable circular orbit (ISCO) versus mass for Skyrmion stars rotating at 290, 360 and 580 Hz respectively (see Table 1).

while the corresponding radii and  $\nu_{ISCO}$  are

$$14.0 \text{ km} < R < 20.0 \text{ km}$$
, (11)

$$0.8 \text{ kHz} < \nu_{\text{ISCO}} < 1.3 \text{ kHz}$$
, (12)

respectively. Our numbers can thus account for the high masses (up to  $1.78 \pm 0.23 M_{\odot}$ ; Orosz, & Kuulkers 1999) determined from LMXBs (see also Miller, Lamb, & Cook 1998). General features of the models discussed in this section are shown in Table 1. A key to all the tables in this paper is as follows:

**Table 1.** Skyrmion stars: Different spin frequencies  $(\nu_s)$ 

$\epsilon_c$	$M_G$	$M_0$	R	$h_+$	$h_{-}$	e	I	j	T/W	$\omega_c/\Omega_c$
$\nu_s=290.0~\mathrm{Hz}$										
$3.0 \times 10^{14}$	1.35	1.46	15.67	0.00	0.00	0.31	2.36	0.49	0.016	0.31
$5.0 \times 10^{14}$	2.28	2.59	16.47	1.93	6.26	0.28	5.09	1.06	0.011	0.49
$6.9 \times 10^{14}$	2.60	3.02	16.13	4.89	9.31	0.24	5.83	1.21	0.009	0.59
$\nu_s=360.0~{ m Hz}$										
$3.0 \times 10^{14}$	1.38	1.48	15.93	0.00	0.00	0.39	2.48	0.64	0.025	0.31
$5.0 \times 10^{14}$	2.30	2.62	16.62	1.69	7.08	0.34	5.24	1.35	0.017	0.50
$6.9 \times 10^{14}$	2.62	3.04	16.24	4.53	10.04	0.28	5.96	1.53	0.014	0.59
$1.0 \times 10^{15}$	2.80	3.29	15.26	7.06	12.18	0.24	5.81	1.50	0.010	0.69
$\nu_s = 580.0 \; \mathrm{Hz}$										
$3.0 \times 10^{14}$	1.53	1.66	17.43	0.00	3.33	0.64	3.25	1.35	0.069	0.34
$5.0 \times 10^{14}$	2.43	2.76	17.42	1.31	10.17	0.53	6.05	2.51	0.048	0.52
$6.9 \times 10^{14}$	2.72	3.16	16.78	3.58	12.72	0.47	6.58	2.73	0.038	0.61
$1.0 \times 10^{15}$	2.86	3.36	15.57	5.85	14.29	0.39	6.18	2.56	0.028	0.70

$\Omega_s$	Star's angular velocity $(10^4 \text{ Hz})$
$\nu_s$	Star's spin frequency, $\nu = \Omega/2\pi$ (Hz)
$\epsilon_c$	Central density (g $cm^{-3}$ )
$M_G$	Gravitational mass $(M_G/M_{\odot})$
$M_0$	Baryonic mass $(M_0/M_{\odot})$
R	Radius of star, measured at equator (km)
$r_{orb}$	Radius of the innermost stable orbit (km)
$h_{+}$	Height from the star surface of innermost sta
	prograde circular orbit (km)
$h_{-}$	Height from the star surface of innermost sta
	retrograde circular orbit (km)
e	Eccentricity
I	Moment of Inertia $(10^{45} \text{ g cm}^2)$
j	Angular momentum $(cJ/GM_{\odot}^2)$
T/ W	Rotational energy to the gravitational energy
$\omega_c/\Omega_c$	Ratio of the inertial frame dragging at the
	center of the star to the rotation rate
$Z_p$	Polar redshift
$Z_f$	Forward redshift
$Z_b$	Backward redshift

To first order in the rotation rate of the star  $(\nu_s < 400 \, \text{Hz})$ , the orbital frequency in the marginally stable orbit is  $\nu_{ISCO} \simeq 2198 \, \text{Hz}(M_{\odot}/M)(1+0.748j(M_{\odot}/M)^2)$  (see Miller, Lamb, & Cook 1998, for example). Consider, as an example, a moderately slowly rotating Skyrmion star,  $\nu = 290 \, \text{Hz}$ , with mass  $M = 2.6 M_{\odot}$ . Using the value of j given in Table 1 we find  $\nu_{ISCO} \sim 9589 \, \text{Hz}$  while the value in the non-rotating case is 8454 Hz (depicted by the dotted line in Fig. 5a).

#### 3.3.1. The case of 4U 1820-30

We first apply our model to 4U 1820-30 which seems to present the strongest experimental evidence for the existence of the marginally stable orbit (Zhang et al. 1998; Kaaret et al. 1999). For  $\nu_{\rm ISCO} \simeq 1060$  Hz as the estimated frequency at the ISCO, and the spin frequency to near 300 Hz, Fig. 5a suggests a mass  $2.35 M_{\odot}$ . The radius is then calculated to be of the order of 16 km. These num-

bers remain to be confirmed from observations and furthet modelling of the system.

### 3.3.2. The case of $4U\ 0614+09$

The highest known QPO has a frequency of 1329 Hz (van Straaten et al. 2000). The frequency of the corresponding star (4U 0614+09) is believed to be near 300 Hz. Simple estimates (van Straaten et al. 2000, §4.4; van der Klis 2000, §5.6) show the difficulty for extremely stiff EOS such as ours to account for the derived range in mass and radius  $(M < 1.9 M_{\odot})$  and R < 15.2 km). We have noted that for our EOS  $\nu_{ISCO} < 1.3$  kHz and R > 14 km. Recent modeling put even more constraints by suggesting a more compact 4U 0614+09 with a radius less than 10 km (Titarchuk & Osherovich 2000).

It is not trivial to account for such numbers in our model unless the 1329 Hz frequency does not actually correspond to the ISCO. Indeed, unlike in the 4U 1820-30 source, there is no obvious saturation of the kilo-hertz QPO with respect to mass accretion indicator in the 4U 0614+09 case (see Fig.4 in van Straaten et al. 2000).

## 4. A comparative study of Skyrmion stars and Neutron stars

In this chapter we compare Skyrmion stars to the more traditional neutron stars. We chose three recent/modern EOSs: the first is described in Baldo, Bombaci, & Burgio (1997) which uses the Argonne v14 (Av14)) (Wiringa, Smith, & Ainsworth 1984) two-body nuclear force; the second uses the Paris two-body nuclear force (Lacombe et al. 1980), implemented in both cases by the Urbana three-body force (TBF) (Carlson, Pandharipande, & Wiringa 1983; Schiavilla, Pandharipande, & Wiringa 1986) while the third one is that developed in Prakash et al. (1997) using a generalized Skyrme-like EOS. As in Datta, Thampan, & Bombaci (1998), we refer to these EOSs as

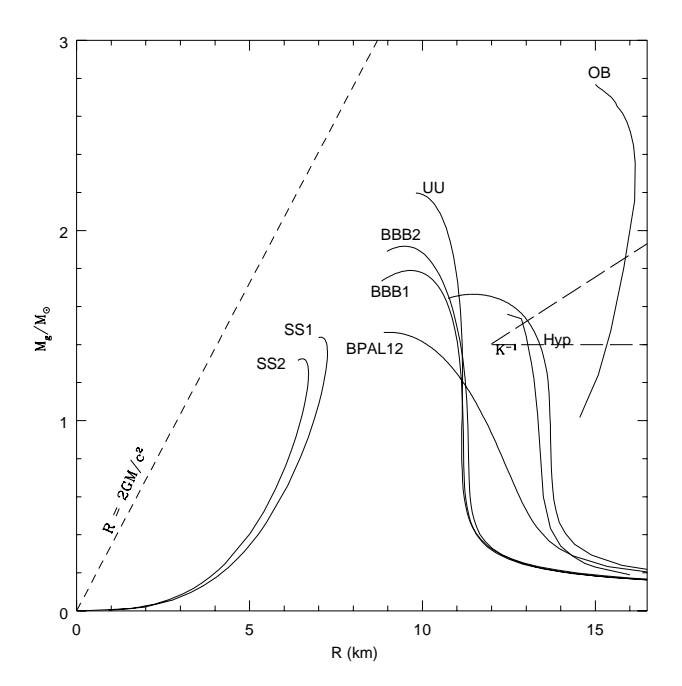


Fig. 6. The M-R relation for non-rotating Skyrmion stars (OB) as compared to theoretical models of non-rotating neutron stars (UU, BBB1, BBB2, BPAL12, Hyp, and K<sup>-1</sup>) and strange stars (SS1 and SS2). The data for the neutron stars and strange stars was kindly provided to us by Li et al. (1999). The Schwarzschild radius  $(2GM/c^2)$  is shown as a dotted line. Inside the triangle is the allowed range of M and R for 4U 1636-53 as modeled in Nath, Strohmayer, & Swank (2001) using fits to X-ray bursts.

BBB1 (Av14+TBF), BBB2 (Paris+TBF) and BPAL32, respectively.

Table 2. Maximum-mass non-rotating models

EOS	$\epsilon_c$	$M_G$	$M_0$	R	$r_{orb}$
BBB1	$3.09 \times 10^{15}$	1.788	2.082	9.646	15.845
BBB2	$3.12 \times 10^{15}$	1.917	2.261	9.519	16.984
BPAL32	$2.67 \times 10^{15}$	1.947	2.263	10.509	17.254
OB	$1.22 \times 10^{15}$	2.797	3.299	14.565	24.743

Table 2 summarizes the non-rotating compact star structure parameters for the EOS models BBB1, BBB2, BPAL32 and ours (OB). The values listed correspond to the maximum stable mass configuration. Note that for this table and the rest of the tables, we consider only the corotating case (the cases where  $r_{\rm orb.}$  is non-existent or inside the star,  $r_{\rm orb.}$  is taken to be the Keplerian orbit radius at the surface of the star). The maximum mass is usually an indicator of the softness/stiffness of the EOS and its values as listed in Table 2 confirms our previous statements that our EOS is stiffer than the standard ones. The consequences of such a stiffness is also illustrated in Table 3 where we list the quantities corresponding to the maximum gravitational mass configurations. It can be seen

that the gravitational mass of the maximum stable rotating Skyrmion star has a value of  $\sim 3.5 M_{\odot}$ , while it is  $\sim 2.4 M_{\odot}$  for the configurations constructed with the other EOS. That is, with our EOS we do not need to go to break up speeds to account for the  $\sim 2.0 M_{\odot}$  mass predicted from analysis of LMXB observational data (Zhang et al. 1996). The values of these same quantities are listed in Table 4 for the maximum angular momentum models leading to similar conclusions.

### 4.1. 4U 1636-53 as a Skyrmion star candidate?

In Fig. 6 we compare the M-R relation for Skyrmion stars (OB) to the theoretical M-R curve obtained using six recent realistic models for the EOS (UU, BBB1, BBB2, BPAL12, Hyp, and  $K^{-1}$ ). The solid curves labeled SS1 and SS2 are for strange stars (the data was kindly provided to us by Li et al. 1999). The triangle depicts the mass-radius constraint from fits to X-ray bursts in 4U 1636-53. Inside the triangle is the allowed range of M and R which satisfies the compactness constraints as modeled in Nath, Strohmayer, & Swank (2001; see their Figure 4), and clearly favoring stiffer EOSs. Our modeled stars (OB) cross the triangle suggestive of 4U 1636-53 as a plausible Skyrmion star candidate. However, one should keep in mind the fact that modern EOSs can be modified as to also cross the triangle (Heiselberg & Hjorth-Jensen 1999).

### 5. Conclusion

With the RNS code, we constructed numerical models of rotating Skyrmion stars for a newly derived EOS of dense matter based on a fluid of Skyrmions. We calculated their masses and radii to be  $0.4 \leq M/M_{\odot} \leq 3.45$  and  $13.0~{\rm km} \leq R \leq 23.0~{\rm km}$ , respectively. The spin period of the maximally rotating configurations are calculated to be  $0.8~{\rm ms} \leq P \leq 2.0~{\rm ms}$ . Owing to the stiffness of the Skyrmion fluid, Skyrmions stars are found to be on average heavier, to show higher equatorial radii, and to rotate slower than theoretical models of neutron stars based on modern realistic EOS.

Skyrmion stars might have little bearing on reality since there is still no guarantee that our EOS (OB) is a plausible representation of matter above nuclear densities. However, our model so far has been successful in reproducing the basic features of compact objects. An interesting consequence of our model, with its plausible applications to QPO systems, is the fact that massive Skyrmion stars (1.8 <  $M/M_{\odot}$  < 3.0) can possess gaps with orbital frequencies in the kHz range (0.8 kHz <  $\nu_{\rm ISCO}$  < 1.3 kHz). These points suggest that the model warrants further study.

Acknowledgements. I am grateful to S. Morsink, M. Butler and G. Kälbermann for encouraging help and valuable discussions. I am also grateful to an anonymous referee for the remarks that helped improve this work. My thanks to N. Stergioulas for making his code available.

Table 3. Maximum-mass rotating models

EOS	$\epsilon_c$	$M_G$	$M_0$	R	$r_{orb}$	e	$\Omega_s$
BBB1	$2.56 \times 10^{15}$	2.135	2.471	13.129	13.490	0.703	1.095
BBB2	$2.82 \times 10^{15}$	2.272	2.653	12.519	13.550	0.687	1.203
BPAL32	$2.27 \times 10^{15}$	2.300	2.657	14.276	14.611	0.699	1.001
OB	$1.03 \times 10^{15}$	3.445	4.034	19.890	21.089	0.837	0.749
	I	j	T/W	$\omega_c/\Omega_c$	$Z_p$	$Z_f$	$Z_b$
	2.428	3.019	0.120	0.764	0.690	-0.330	1.975
	2.539	3.469	0.123	0.825	0.849	-0.349	2.483
	3.005	3.416	0.113	0.771	0.679	-0.328	1.933
	9.982	8.507	0.144	0.777	0.777	-0.342	2.287

Table 4. Maximum angular momentum models

EOS	$\epsilon_c$	$M_G$	$M_0$	R	$r_{orb}$	e	$\Omega_s$
BBB1	$2.44 \times 10^{15}$	2.133	2.468	13.264	13.558	0.706	1.079
BBB2	$2.82 \times 10^{15}$	2.272	2.653	12.519	13.550	0.687	1.203
BPAL32	$2.14 \times 10^{15}$	2.299	2.655	14.481	14.713	0.702	0.981
OB	$9.00 \times 10^{14}$	3.435	4.017	20.549	21.498	0.840	0.715
	I	j	T/W	$\omega_c/\Omega_c$	$Z_p$	$Z_f$	$Z_b$
	2.465	3.021	0.120	0.756	0.677	-0.328	1.935
	2.539	3.469	0.123	0.825	0.849	-0.349	2.483
	3.070	3.419	0.114	0.760	0.661	-0.326	1.881
	10.52	8.560	0.146	0.751	0.728	-0.355	2.133

### References

Andersson, N., Kokkotas, K., & Schutz, B. 1999, ApJ, 510, 846 Baldo, M., Bombaci, I., & Burgio G. F. 1997, A&A 328, 274 Bardeen, J. M. 1970, ApJ, 162, 71

Bardeen, J. M., & Wagoner R. V. 1971, ApJ, 167, 359 Bardeen, J. M. 1972, ApJ, 178, 347

Baym, G., Pethick, C. J., & Sutherland, P. G. 1971, ApJ, 170, 299

Bonazzola, S., Frieben, J., & Gourgoulhon, E. 1995, ApJ, 460, 379

Butterworth, E. M., & Ipser, J. R. 1976, ApJ, 204, 200
Carlson, J., Pandharipande, V. R., & Wiringa, R. B. 1983,
Nucl. Phys. A401, 59

Datta, B., Thampan, A. V., & Bombaci, I. 1998, A&A, 334, 943

Friedman, J. L. & Schutz, B. F. 1978, ApJ, 222, 281

Friedman, J. L., & Ipser J. R., 1992, Phil. Trans. R. Soc. Lond. A, 340,391

Friedman, J. L., & Morsink, S. M., 1998, ApJ, 502, 714

Glendenning, N. K. 1997, Compact Stars (Springer-Verlag, New York)

Hænsel, P., & Zdunik, J.L. 1989, Nature, 340, 617

Hænsel, P., Salgado, M., & Bonazzola, S. 1995, A&A, 296, 745 617

 Heiselberg, H., & Hjorth-Jensen, M. 1999, ApJ, 525, L45
 Heusler, M., Droz, S., & Straumann, N. 1992, Phys. Lett. B 285, 21

Kaaret, P., Piraino, S., Bloser, P. F., Ford, E. C., Grindlay, J. E., Santangelo, A., Smale, A. P., & Zhang, W. 1999, ApJ, 520, L37

Kälbermann, G. 1997, Nucl. Phys., A612, 359

van der Klis, M. 1998, In: the Many Faces of Neutron Stars, ed. R. Buccheri, J. van Paradijs, & M. A. Alpar (Dordrecht: Kluwer), 337

van der Klis, M. 2000, ARA&A, 38, 717

Komatsu, H., Eriguchi, Y., & Hachisu, I. 1989, MNRAS, 237, 355

Lacombe, M., Loiseau, B., Richard, J. M., et al. 1980, Phys. Rev. C, 21, 861

Li, X-D., Ray, S., Dey, J., Dey, M., & Bombaci, I. 1999, ApJL, 527, L51

Lindblom, L. 1984, ApJ, 278, 364

Miller, M. C., Lamb, F. K., & Psaltis, D. 1998, ApJ, 508, 791
Miller, M. C., Lamb, F. K., & Cook, G. B. 1998, ApJ, 509, 793
Morsink, S. M., Stergioulas, N., & Blattnig, S. R. 1999, ApJ, 510, 854

Nath, N. R., Strohmayer, T. E., & Swank, J. H. 2001, astro-ph/0102421

Ouyed, R., & Butler, M. 1999, ApJ, 522, 453 (OB)

Orosz, J. A., & Kuulkers, E. 1999, MNRAS, 305, 132

Prakash, M., Bombaci, I., Prakash, M., et al. 1997, Phys. Rep.

Schiavilla, R., Pandharipande, V. R., & Wiringa, R. B. 1986, Nucl. Phys. A449, 219

Skyrme, T. H. R. 1962a, Proc. R. Soc. London Ser., A260, 127 Skyrme, T. H. R. 1962b, Nucl. Phys. , 31, 556

Stergioulas, N., & Friedman, J. L. 1995, ApJ, 444, 306

Stergioulas, N., & Friedman, J. L. 1998, ApJ, 492, 301

van Straaten, S. et al., 2000, ApJ, 540, 1049

Titarchuk, L., & Osherovich, V. 2000, ApJ, 537, L39

Weber, F. & Glendenning, N. K. 1992, ApJ, 390, 541

Wiringa, R. B., Smith R. A., & Ainsworth T. L. 1984, Phys. Rev. C29, 1207

Zhang, W., Lapidus I., White N. E., & Titarchuk L. 1996, ApJ 469, L17

Zhang, W., Smale, P., Strohmayer, T. E., & Swank, J. H. 1998, ApJ, 500, L171